



ELSEVIER

SCIENCE @ DIRECT®

PHYSICS LETTERS B

Physics Letters B 598 (2004) 47–54

www.elsevier.com/locate/physletb

Measurement of the tensor analyzing power T_{20} in the $dd \rightarrow {}^3\text{He}n$ and $dd \rightarrow {}^3\text{H}p$ at intermediate energies and at zero degree

V.P. Ladygin^h, T. Uesaka^a, T. Saito^b, M. Hatano^b, A.Yu. Isupov^h, H. Kato^b,
N.B. Ladygina^h, Y. Maeda^a, A.I. Malakhov^h, J. Nishikawa^d, T. Ohnishi^c,
H. Okamura^e, S.G. Reznikov^h, H. Sakai^{a,b}, N. Sakamoto^c, S. Sakoda^b,
Y. Satou^f, K. Sekiguchi^c, K. Suda^a, A. Tamii^f, N. Uchigashima^b, K. Yako^b

^a Center for Nuclear Study, University of Tokyo, Bunkyo, Tokyo 113-0033, Japan

^b Department of Physics, University of Tokyo, Bunkyo, Tokyo 113-0033, Japan

^c RIKEN, Wako, Saitama 351-0198, Japan

^d Department of Physics, Saitama University, Urawa 338-8570, Japan

^e CYRIC, Tohoku University, Sendai, Miyagi 980-8578, Japan

^f Research Center for Nuclear Physics, Osaka University, Ibaraki 567-0047, Japan

^g Department of Physics, Tokyo Institute of Technology, Tokyo 152-8551, Japan

^h LHE-JINR, 141980 Dubna, Moscow region, Russia

Received 2 April 2004; accepted 4 August 2004

Editor: J.P. Schiffer

Abstract

The data on the tensor analyzing power T_{20} in the $dd \rightarrow {}^3\text{He}n$ and $dd \rightarrow {}^3\text{H}p$ reactions obtained at 140–270 and 140–200 MeV of the deuteron kinetic energy, respectively, and at zero degree were measured at RIKEN Accelerator Research Facility. The observed positive sign of T_{20} clearly demonstrates the sensitivity to the D/S wave ratios in the ${}^3\text{He}$ and ${}^3\text{H}$ in the energy domain of the measurements. The T_{20} data for the ${}^3\text{He}-n$ and ${}^3\text{H}-p$ channels are in agreement within experimental accuracy.

© 2004 Elsevier B.V. Open access under [CC BY license](https://creativecommons.org/licenses/by/4.0/).

PACS: 24.70.+s; 21.45.+v

Keywords: Tensor analyzing power; Spin structure; Deuteron; Triton; ${}^3\text{He}$

E-mail address: ladygin@sunhe.jinr.ru (V.P. Ladygin).

0370-2693 © 2004 Elsevier B.V. Open access under [CC BY license](https://creativecommons.org/licenses/by/4.0/).

doi:10.1016/j.physletb.2004.08.002

The spin structure of the light nuclei has been extensively investigated during the last decades using both electromagnetic and hadronic probes. The main purposes of these studies at intermediate and high energies are to obtain the possible effects in the high-momentum components of light nuclei due to the relativity and the manifestation of non-nucleonic degrees of freedom. Three nucleon bound states are of particular interest, because even a fundamental constant as the binding energy in the system cannot be reproduced by calculations with modern pairwise nucleon–nucleon potentials [1]. Since the binding energy is known to have a strong relation to the strength of spin-dependent forces such as tensor forces and/or three-nucleon forces, an experimental study of the spin structure of three-nucleon bound system is crucial to gain a clue to understand the source of the missing energy.

The non-relativistic Faddeev calculations [2] for three-nucleon bound state predict that the dominant components of the ${}^3\text{He}$ ground state are a symmetric S -state, where the ${}^3\text{He}$ spin due to the neutron and two protons are in a spin singlet state and a D -state, where all three nucleon spins are oriented opposite to the ${}^3\text{He}$ spin. The S -state is found to dominate at small momenta while D -state dominates at large momenta. The relative sign of D - and S -wave in the momentum space is positive at small and moderate nucleon momenta [3].

The sensitivity to the different components of ${}^3\text{He}$ can be observed in polarization observables in both hadronic and electromagnetic processes.

Polarized electron scattering on polarized ${}^3\text{He}$ target, ${}^3\overline{\text{He}}(\vec{e}, e')X$, can be used to study the different components of the ${}^3\text{He}$ wave function [2]. However, it is necessary to take into account final state interaction (FSI) and meson exchange currents (MEC) in addition to the plane wave impulse approximation (PWIA) to describe the experimental results [4] obtained at different relative orientations of electron and ${}^3\text{He}$ spins. Recent CEBAF data on the transverse asymmetry $A_{T'}$ [5] at Q^2 values of 0.1 and 0.2 GeV/ c^2 have been described using full Faddeev calculation with the MEC effects.

The ${}^3\overline{\text{He}}(\vec{p}, 2p)$ and ${}^3\overline{\text{He}}(\vec{p}, pn)$ breakup reactions were studied at TRIUMF in quasielastic kinematics at 200 [6] and 290 MeV [7] of incident proton energy. In the last experiment, spin observables A_{no} ,

A_{on} and A_{nn} were measured up to $q \sim 190$ and ~ 80 MeV/ c for ${}^3\overline{\text{He}}(\vec{p}, 2p)$ and ${}^3\overline{\text{He}}(\vec{p}, pn)$ reactions, respectively. The results indicate that analyzing powers A_{no} , A_{on} and A_{nn} are close to the PWIA calculations for the ${}^3\overline{\text{He}}(\vec{p}, 2p)$ reaction, while for the ${}^3\overline{\text{He}}(\vec{p}, pn)$ there is a strong disagreement with these predictions. The same observables were recently measured at 197 MeV at IUCF Cooler Ring [8] up to $q \sim 400$ MeV/ c . It was observed that the polarization of the neutron and proton at zero nucleon momentum in ${}^3\text{He}$ are $P_n \sim 0.98$ and $P_p \sim -0.16$, respectively, that is in good agreement with the Faddeev calculations [2]. However, at higher momenta there is the discrepancy, which can be due to the uncertainty of the theoretical calculations, as well as to large rescattering effects.

One nucleon exchange (ONE) reactions, like $dp \rightarrow pd$, $d{}^3\text{He} \rightarrow p{}^4\text{He}$ or $d{}^3\text{He} \rightarrow {}^3\text{He}d$, are the simplest processes with large momentum transfer and, therefore, can be used as an effective tool to investigate the structure of the deuteron and ${}^3\text{He}$ at short distances. In the framework of the ONE approximation [9] the polarization observables of the above reactions are expressed in terms of the D/S -wave ratios of these nuclei. For instance, tensor analyzing power T_{20} for the $dp \rightarrow pd$ reaction in the collinear geometry is expressed in terms of D/S wave ratio, r , of the deuteron in the momentum space [9]

$$T_{20} = \frac{2\sqrt{2}r - r^2}{\sqrt{2}(1 + r^2)}. \quad (1)$$

A significant amount of the data devoted to the investigation of the deuteron and ${}^3\text{He}$ (${}^3\text{H}$) spin structure at short distances have been accumulated in the last years. Recently, the tensor analyzing power T_{20} and polarization transfer coefficients in backward elastic scattering, $dp \rightarrow pd$, have been measured at Saclay, Dubna and RIKEN [10–13]. Another binary reaction, $d{}^3\text{He} \rightarrow p{}^4\text{He}$, has been investigated at RIKEN using both polarized deuteron and ${}^3\text{He}$ up to 270 MeV [14–16]. All the data show the sensitivity to the deuteron spin structure at short distances. For instance, T_{20} for both $dp \rightarrow pd$ [10,12,13] and $d{}^3\text{He} \rightarrow p{}^4\text{He}$ [15,16] reactions at intermediate energies has a large negative value reflecting the negative sign of the D/S -wave ratio in the deuteron in the momentum space.

Concerning the ${}^3\text{He}$ spin structure, the tensor analyzing power T_{20} in the $d^3\text{He}$ backward elastic scattering has been measured at 140, 200 and 270 MeV [17]. The sign of T_{20} is found to be positive in accordance with the positive sign of D/S -wave ratio in the ${}^3\text{He}$ [3].

The data sensitive to the three-nucleon bound state spin structure are still scarce, and, new polarization data, especially, at short distances is of great importance. The $dd \rightarrow {}^3\text{H}p({}^3\text{He}n)$ process is the simplest ONE reaction where the three nucleon structure is relevant. The theoretical analysis of the polarization phenomena for this reaction in the collinear geometry has been performed [18,19]. It has been shown that the tensor analyzing power T_{20} due to polarization of the incident deuteron can be expressed in the terms of the D/S -wave ratio in the ${}^3\text{H}({}^3\text{He})$, when three-nucleon bound state is emitted in the forward direction in the cms. A new experiment has been proposed [20] to measure the energy and angular dependence of the tensor analyzing powers in the $dd \rightarrow {}^3\text{H}p({}^3\text{He}n)$ process at RIKEN.

In this Letter the data on the tensor analyzing power T_{20} due to the incident deuteron polarization in the $dd \rightarrow {}^3\text{He}(0^\circ)n$ and $dd \rightarrow {}^3\text{H}(0^\circ)p$ reactions at 140, 200 and 270 MeV of the deuteron kinetic energy are presented.

The experiment has been performed at RIKEN accelerator research facility (RARF). A polarized deuteron beam was produced by the high-intensity polarized ion source (PIS) [21] and accelerated by AVF and ring cyclotrons up to the required energy. In the present experiment the data were taken for the vector and tensor polarization modes noted by the theoretical maximum polarization of $(p_z, p_{zz}) = (0, 0), (0, -2), (-2/3, 0)$ and $(1/3, 1)$. The polarization modes were cycled every 5 seconds by switching the RF transition units of the PIS. The direction of the beam polarization axis was controlled with a Wien filter located at the exit of the PIS. It was perpendicular to the scattering plane or pointing sideways in the scattering plane when measuring A_{yy} or A_{xx} , respectively.

The polarization of the beam has been measured with two beam-line polarimeters based on the asymmetry measurements in dp -elastic scattering, which has large values of tensor and vector analyzing powers [12,22]. New data of the analyzing powers for dp -elastic scattering at 140 and 270 MeV were used

Table 1

Tensor polarization of the beam for the modes $(0, -2)$ and $(1/3, 1)$

Energy, MeV	Mode (0, -2)	Mode (1/3, 1)
270	-1.256 ± 0.023	0.766 ± 0.016
200	-0.828 ± 0.016	0.585 ± 0.014
140	-0.285 ± 0.006	0.210 ± 0.005

in the analysis. The values were obtained for the polarized deuteron beam, the absolute polarization of which was calibrated via the ${}^{12}\text{C}(d, \alpha){}^{10}\text{B}^*[2^+]$ reaction [23]. The thin CH_2 sheet was the target for both polarimeters. Each polarimeter consisted of four pairs of 1 cm thick plastic scintillators placed symmetrically in left, right, up and down directions. The scattered deuterons and recoil protons were detected in a kinematical coincidence.

The first polarimeter installed downstream of the ring cyclotron was used for the monitoring of beam polarization during the data taking. The second one located in front of the scattering chamber in the experimental room was used to measure the polarization before and after run. The beam polarization for each polarization state of the PIS was taken as weighted average of the values obtained using both polarimeters.

The results on the beam tensor polarization for the modes $(0, -2)$ and $(1/3, 1)$ are given in Table 1. The systematic error due to uncertainties of the analyzing powers of the polarimetries and the statistical error in the polarization measurement are added in quadrature. The systematic error does not exceed $\sim 2\%$ at all the energies. Actual values of the beam polarization, for example, for the mode $(1/3, 1)$ were $\sim 75\%$, $\sim 50\%$ and $\sim 25\%$ of the theoretical maximum values at 270, 200 and 140 MeV, respectively. The decreases of the polarization at 200 and 140 MeV are due to an aging effect of the PIS.

SMART (swinger and magnetic analyzer with a rotator and a twister) spectrograph [24] has been used for the measurements. $(Q-Q-D-Q-D)$. A CD_2 thin sheet [26] placed in the scattering chamber of the SMART has been used as a deuterium target. The measurements on CD_2 and carbon targets were made for each setup setting to obtain the contribution from deuterium via the CD_2 -C subtraction. The thicknesses of the CD_2 and carbon targets used were 54 mg/cm^2 and 34 mg/cm^2 , respectively. The measurement of

the particle's momentum and separation from the primary beam was achieved by the magnetic system of SMART spectrograph consisting of two dipole and three quadrupole magnets. The beam intensity monitored by the Faraday cup located in the first dipole magnet was about 1–2 nA during the experiment. The detection solid angle was 10^{-2} sr.

The detection system of SMART consisted of a multiwire drift chamber (MWDC) and three plastic scintillation counters. The MWDC information was used to reconstruct the particles trajectories in the focal plane. Three plastic scintillation counters BICRON BC-408 with the size $180 \text{ mm}^H \times 800 \text{ mm}^W \times 5 \text{ mm}^T$ were used in coincidence for the trigger and to provide the information about time-of-flight and energy losses of the particles. The photo-tubes Hamamatsu H1161 were placed on the both sides of the scintillators via light guides. The size of the scintillation counters was large enough to cover the momentum and angular ranges of interest in the present study. The live time of DAQ system [25] was more than 80% at the trigger rate of few thousands per second.

The time difference between the trigger signal and the radio-frequency signal of cyclotron was used as the time-of-flight information (TOF). The distance between the target and the detection point is about 17 m, which is enough to separate tritons, deuterons and protons with the same momentum from the TOF. Pulse heights of the plastic scintillation counters were used to select the particle of interest at the trigger level. In the cases of ${}^3\text{He}$ and ${}^3\text{H}$ detection, protons and deuterons were partly suppressed by raising threshold levels of the discriminators. The fraction of the event rate for undesired particles are as small as $\sim 40\%$ and $\sim 0.5\%$ for ${}^3\text{He}$ and ${}^3\text{H}$ detection, respectively. The admixtures of background events were almost completely eliminated by a software cut in the offline analysis.

The typical track reconstruction efficiency of the MWDC was better than 99%. The ion-optical parameters of SMART was used to obtain the information on the momentum of the particle and emission angle from the target from the track information. The obtained energy resolution was ~ 300 keV.

In the experiment the data for ${}^3\text{He}-n$ channels have been obtained at 140, 200 and 270 MeV, while for the ${}^3\text{H}-p$ channel only at 140 and 200 MeV. This is be-

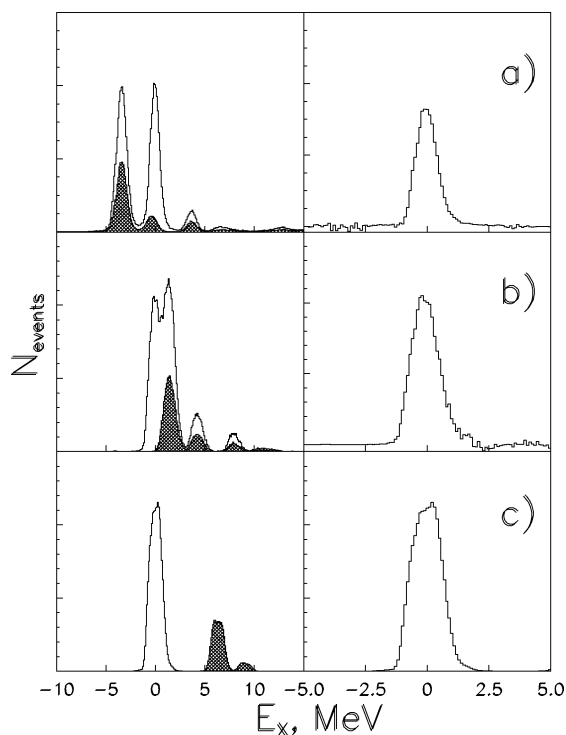


Fig. 1. $\text{CD}_2\text{-C}$ subtraction for the $dd \rightarrow {}^3\text{He}(0^\circ)n$ channel: (a) at 270 MeV, (b) at 200 MeV and (c) at 140 MeV. The open and shadowed histograms in the left panels correspond to the yields from CD_2 and carbon targets, respectively. The right panels demonstrate the quality of the $\text{CD}_2\text{-C}$ subtraction.

cause the momentum of the ${}^3\text{H}$ at 270 MeV is higher than the maximum rigidity of SMART [24].

The quality of the $\text{CD}_2\text{-C}$ subtraction procedure for the $dd \rightarrow {}^3\text{He}(0^\circ)n$ reaction at 270, 200 and 140 MeV is demonstrated in Fig. 1(a), (b) and (c), respectively. The spectra are plotted versus excitation energy E_X defined as following:

$$E_X = \sqrt{(E_0 - E_{3N})^2 - (\mathbf{P}_0 - \mathbf{P}_{3N})^2} - M_N, \quad (2)$$

where \mathbf{P}_0 is the incident momentum; $E_0 = 2M_d + T_d$ is the total initial energy; E_{3N} and \mathbf{P}_{3N} are the energy and the momentum of the three-nucleon system, respectively; M_N is the nucleon mass. The left panels represent the relative yields from CD_2 and carbon targets shown by the open and shadowed histograms, respectively. Peaks at $E_X = 0$ MeV correspond to ${}^3\text{He}$ from the $dd \rightarrow {}^3\text{He}n$ reaction. The right panels show the spectra after subtraction of carbon events with a normalization due to a beam charge, a target thickness,

and a dead time correction. It is clearly demonstrated that the subtraction procedure has been made successfully.

For the ${}^3\text{H}$ detection case the yield from carbon under peak at $E_X = 0$ MeV is negligibly small. The peak for the binary reaction on deuterium, $dd \rightarrow {}^3\text{H}p$, is separated from the peaks for the reaction $d^{12}\text{C} \rightarrow {}^3\text{H}X$ by ~ 5 and ~ 10 MeV at 200 and 140 MeV, respectively.

The polarization dependent yields at 0° were by integrating events in symmetrical polar angle acceptance $\theta \leq 1.4^\circ$. In this case the dependence of the yield on the azimuthal angle completely averages out.

Only the events for the unpolarized mode (0, 0) and the two polarization modes with the tensor polarization, (0, -2) and (1/3, 1) [21] were used in the analysis.

Tensor analyzing power T_{20} was calculated for each polarization mode from the following expression

$$T_{20} = -\frac{2\sqrt{2}}{p_{zz}} \left(\frac{\sigma_{\text{pol}}}{\sigma_0} - 1 \right), \quad (3)$$

where p_{zz} is the corresponding tensor polarization of the beam, σ_{pol} and σ_0 are yields in the polarized and the unpolarized modes obtained after $\text{CD}_2\text{-C}$ subtraction and corrected for the dead-time effect, the detection efficiency and the beam intensity. Since the polarization modes were cycled every 5 seconds, the systematic uncertainty due to any time-dependent effects such as deuterium loss from the CD_2 target due to beam irradiation can be neglected. The analyzing power T_{20} was obtained as a weighted average for two polarization modes.

The systematic uncertainty in T_{20} due to the $\text{CD}_2\text{-C}$ subtraction procedure was found to be less than 1% at 200 MeV for the ${}^3\text{He}n$ channel. Since the admixture of events from carbon under binary reaction peak for the ${}^3\text{H}p$ channel was as small as 10^{-3} , the systematic error in T_{20} due to the subtraction procedure for this channel was negligible.

The false asymmetry arising from the misalignment of the beam axis and the axis of SMART was estimated from data in the pure vector mode, $(-2/3, 0)$. At a zero degree due to rotation symmetry the asymmetry $(\sigma_{\text{pol}}/\sigma_0 - 1)$ should be equal to zero in this mode. The false asymmetry is found to be not more than 1%.

Table 2

Tensor analyzing power T_{20} in the $dd \rightarrow {}^3\text{He}n$ and $dd \rightarrow {}^3\text{H}p$ reactions

Energy, MeV	Reaction	T_{20}	ΔT_{20}
140	$dd \rightarrow {}^3\text{He}n$	0.112	0.019
140	$dd \rightarrow {}^3\text{H}p$	0.082	0.018
200	$dd \rightarrow {}^3\text{He}n$	0.172	0.020
200	$dd \rightarrow {}^3\text{H}p$	0.165	0.018
270	$dd \rightarrow {}^3\text{He}n$	0.300	0.013

The effect of the smearing due to finite acceptance was estimated from the angular dependences of the tensor analyzing power within polar angle acceptance $\theta \leq 4.0^\circ$. The angular dependence was fitted by the function $p_0 + p_1 \cdot \theta^2$. The effect of T_{20} smearing obtained by the integration of the above function within range $\theta \leq 1.4^\circ$ was found to be less than 1% for all the energies and all the reaction channels.

The results on the tensor analyzing power T_{20} for the $dd \rightarrow {}^3\text{He}(0^\circ)n$ and $dd \rightarrow {}^3\text{H}(0^\circ)p$ reactions are given in Table 2. The systematic error due to uncertainty in the beam polarization and the statistical error are added in quadrature. This systematic error is approximately $\sim 2\%$ for all the energies (see Table 1).

These data are plotted as a function of an incident deuteron momentum in Fig. 2. The open triangles and full circles correspond to the ${}^3\text{H}-p$ and ${}^3\text{He}-n$ channels, respectively. The T_{20} values obtained for the both charge symmetrical ${}^3\text{H}-p$ and ${}^3\text{He}-n$ channels at 140 and 200 MeV in this experiment are in good agreement to each other within achieved experimental accuracy. No evidence of charge symmetry breaking is found in these processes.

The positive sign of T_{20} values is in a striking contrast to the negative T_{20} for $dp \rightarrow pd$ or other reactions where the deuteron structure is relevant. It is also shown that the amplitude of T_{20} increases with the momentum. This behavior can be understood from the increasing D/S wave ratio in the ${}^3\text{He}({}^3\text{H})$ with the help of ONE.

Within the ONE approximation, tensor analyzing power T_{20} for the $dd \rightarrow {}^3\text{H}p({}^3\text{He}n)$ reaction in the collinear geometry is expressed in terms of D and S wave ratio r of the ${}^3\text{H}({}^3\text{He})$ [18–20] (see expression (1)). The positive sign of T_{20} in the explored energy domain reflects the positive sign of the D/S wave ratio in the ${}^3\text{He}({}^3\text{H})$ in the momentum space [2,3]. In

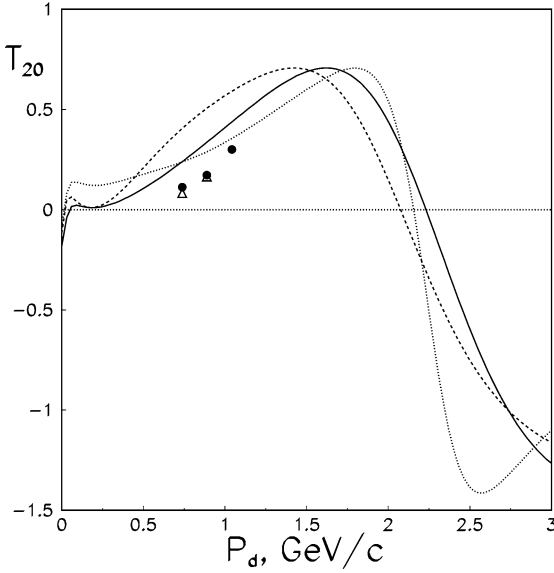


Fig. 2. Tensor analyzing power T_{20} in the $dd \rightarrow {}^3\text{He}n$ (solid circles) and $dd \rightarrow {}^3\text{He}p$ (open triangles) reactions in collinear geometry versus incident momentum of deuteron. The solid, dashed and dotted curves are the results of the non-relativistic ONE calculations [20] for the forward emission of the ${}^3\text{He}({}^3\text{H})$ in the cms, using Urbana [27], Paris [28] and RSC [29] ${}^3\text{He}$ wave functions, respectively. Paris deuteron wave function [31] was used for the deuteron structure description.

this respect one can conclude that our data are sensitive to the D -state in the ${}^3\text{He}({}^3\text{H})$.

The solid, dashed and dotted curves in Fig. 2 are the results of non-relativistic ONE calculations [20] using Urbana [27], Paris [28] and RSC [29] (with the parametrization from [30]) wave functions of ${}^3\text{He}$. For the deuteron wave function, Paris parametrization [31] was used. It should be noted, however, that T_{20} is insensitive to the deuteron structure in the conditions of the experiment [18–20]. The data are in a qualitative agreement with the ONE calculations [20].

The behavior of our data is consistent with the behaviour of T_{20} for other reactions where the ${}^3\text{He}$ spin structure is relevant. In Fig. 3 the data on T_{20} in the $dd \rightarrow {}^3\text{He}(0^0)n$ are plotted along with the data obtained for the $d^3\text{He} \rightarrow {}^3\text{He}d$ reaction [17] as a function of the internal momentum k defined as follows [32]:

$$k = \left(\alpha - \frac{1}{2} \right) \cdot \epsilon + \frac{m_d^2 - m_p^2}{\epsilon},$$

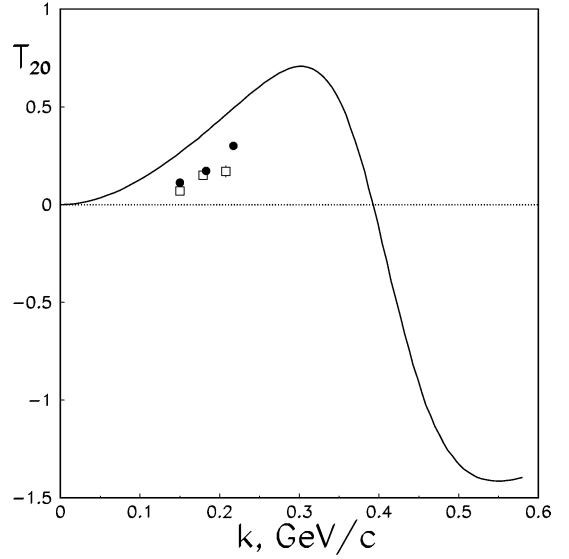


Fig. 3. Tensor analyzing power T_{20} in the $dd \rightarrow {}^3\text{He}n$ (solid circles) and $d^3\text{He} \rightarrow {}^3\text{He}d$ (open squares) [17] reactions versus internal momentum k . The solid curve is the result of the ONE calculations using Urbana ${}^3\text{He}$ wave function [27].

$$\epsilon = \sqrt{\frac{m_p^2 \cdot (1 - \alpha) + m_d^2 \cdot \alpha}{\alpha \cdot (1 - \alpha)}},$$

$$\alpha = \frac{\sqrt{m_p^2 + q^2} + q}{m_\tau}, \quad (4)$$

where the relativistic effects are taken into account by the minimal relativization scheme [32]. In Eq. (4), m_p , m_d and m_τ are the masses of proton, deuteron and ${}^3\text{He}$, respectively, q is the momentum of proton in the rest frame of ${}^3\text{He}$.

The data for the both processes demonstrate the universality in the k -behaviour. The solid curve is the result of ONE calculation using Urbana ${}^3\text{He}$ wave function [27] according to Eq. (1).

The discrepancy between the data and the calculations found in Fig. 3 can be due both to the contribution from the reaction mechanism other than ONE and to the nonadequate description of the short-range ${}^3\text{He}$ spin structure. Concerning the reaction mechanism, the virtual excitation to the other channels, for example, excitation to Δ -isobar, is considered to be the most important. This effect is taken into account phenomenologically in Ref. [17] to reproduce the energy dependence of T_{20} for the $d^3\text{He} \rightarrow {}^3\text{He}d$ process. The microscopic calculation by Laget et al. [28] shows that

the coherent sum of ONE and the Δ -isobar excitation reproduces the cross section for the $dd \rightarrow {}^3\text{He}n$ reaction at GeV energies reasonably. The calculation predicts that the Δ -isobar contribution to the cross section is 10% at most in the energy region lower than 300 MeV.

Therefore, the $dd \rightarrow {}^3\text{He}n$ reaction at the energy of the present study can be described by the dominating ONE process and a small contribution from the Δ -isobar excitation. Thus it is expected that the uncertainty in the reaction mechanism is still small to explain the discrepancy between the data and the ONE calculation. In this case, the disagreement between the data and ONE is mainly due to the ${}^3\text{He}$ spin structure. There still remains, however, another possibility that reaction mechanism other than Δ -isobar excitation can affect more largely to the polarization data than to the cross section data. To understand the T_{20} data presented here, further theoretical investigations of the short-range ${}^3\text{He}$ spin structure as well as the reaction mechanism of the $dd \rightarrow {}^3\text{He}n$ process are clearly needed.

The extension of the T_{20} measurements to the higher energies, namely to larger internal momenta, is of great interest. In particular, the measurement of T_{20} in the vicinity of $k \sim 0.4$ GeV/ c , where the changing of the T_{20} sign is expected, could distinguish different models of the short range ${}^3\text{He}$ spin structure description.

The results can be summarized as follows.

The data on the tensor analyzing power T_{20} in the $dd \rightarrow {}^3\text{H}p$ and $dd \rightarrow {}^3\text{He}n$ reactions at intermediate energies and in collinear geometry are obtained. The sign of T_{20} is positive being in the agreement with the results on T_{20} in the $d{}^3\text{He} \rightarrow {}^3\text{He}d$ reaction [17], on the one hand, and with the ONE calculations using standard ${}^3\text{He}$ wave functions, on the other hand.

According to the calculations [28] the $dd \rightarrow {}^3\text{He}n$ reaction is dominated by ONE at these energies. The Δ -isobar contribution is less than 10% at energies lower than 300 MeV [28]. In general, ONE reproduces qualitatively the global feature of the T_{20} energy dependence, namely, the sign and increasing amplitude of the T_{20} value with the energy in the range of our experiment. The deviation of the experimental data from the ONE calculations can be explained as due to the nonadequate description of the short range ${}^3\text{He}$ spin structure within the theoretical model considered here.

On the other hand, it is possible that the other than above considered reaction mechanisms can affect to the polarization data. To improve the description of the obtained data further theoretical calculations are required. In this context, our data are important to study the $dd \rightarrow {}^3\text{He}n$ reaction as a probe to explore the short range spin structure of three nucleon bound state.

Acknowledgements

The authors express their thanks to the staff of RARF for providing of excellent conditions for the R308n experiment. They are grateful to H. Kumasaka, R. Suzuki and R. Taki for their help during experiment. Russian part of collaboration thanks RIKEN Directorate for kind hospitality during the experiment. The work has been supported in part by the JINR-Bulgaria grants for 2001 and 2002 years and by the Russian Foundation for Fundamental Research (grant No. 04-02-17107).

References

- [1] W. Glöckle, H. Witala, D. Hüber, H. Kamada, J. Golak, Phys. Rep. 274 (1996) 107.
- [2] B. Blankleider, R.M. Woloshyn, Phys. Rev. C 29 (1984) 538; J.L. Friar, B.F. Gibson, G.L. Payne, A.M. Bernstein, T.E. Chupp, Phys. Rev. C 42 (1990) 2310; R.-W. Schulze, P.U. Sauer, Phys. Rev. C 48 (1993) 38.
- [3] A.M. Eiro, F.D. Santos, J. Phys. G: Nucl. Phys. 16 (1990) 1139.
- [4] C.E. Woodward, et al., Phys. Rev. Lett. 65 (1990) 698; C.E. Jones-Woodward, et al., Phys. Rev. C 44 (1991) R571; A.K. Thompson, et al., Phys. Rev. Lett. 68 (1992) 2901; M. Meyerhoff, et al., Phys. Lett. B 327 (1994) 201.
- [5] W. Xu, et al., Phys. Rev. Lett. 85 (2000) 2900.
- [6] E.J. Brash, et al., Phys. Rev. C 47 (1993) 2064.
- [7] A. Rahav, et al., Phys. Lett. B 275 (1992) 259; A. Rahav, et al., Phys. Rev. C 46 (1992) 1167.
- [8] M.A. Miller, et al., Phys. Rev. Lett. 74 (1995) 502.
- [9] S.S. Vasan, Phys. Rev. D 8 (1973) 4092; V.A. Karmanov, Yad. Fiz. 34 (1981) 1020.
- [10] V. Punjabi, et al., Phys. Lett. B 350 (1995) 178.
- [11] L.S. Azhgirey, et al., Phys. Lett. B 391 (1997) 22; L.S. Azhgirey, et al., Yad. Fiz. 61 (1998) 494.
- [12] K. Sekiguchi, et al., Phys. Rev. C 65 (2002) 034003.
- [13] H. Sakai, et al., Phys. Rev. Lett. 84 (2000) 5288.
- [14] T. Uesaka, et al., Phys. Lett. B 467 (1999) 199.
- [15] T. Uesaka, et al., Few-Body Systems Suppl. 12 (2000) 497.
- [16] T. Uesaka, et al., Phys. Lett. B 533 (2002) 1.

- [17] M. Tanifuji, et al., *Phys. Rev. C* 61 (2000) 024602.
- [18] V.P. Ladygin, N.B. Ladygina, *Phys. At. Nucl.* 59 (1996) 789.
- [19] V.P. Ladygin, N.B. Ladygina, *Nuovo Cimento A* 112 (1999) 855.
- [20] V.P. Ladygin, N.B. Ladygina, H. Sakai, T. Uesaka, *Part. Nucl. Lett.* 3 (2000) 74.
- [21] H. Okamura, et al., *AIP Conf. Proc.* 293 (1993) 84.
- [22] N. Sakamoto, et al., *Phys. Lett. B* 367 (1996) 60.
- [23] K. Suda, et al., *AIP Conf. Proc.* 570 (2001) 806;
K. Suda, et al., *RIKEN Accel. Prog. Rep.* 35 (2002) 174.
- [24] T. Ichihara, et al., *Nucl. Phys. A* 569 (1994) 287c.
- [25] H. Okamura, *Nucl. Instrum. Methods Phys. Res. A* 443 (2000) 194.
- [26] Y. Maeda, H. Sakai, K. Hatanaka, A. Tamii, *Nucl. Instrum. Methods Phys. Res. A* 490 (2002) 518.
- [27] R. Schiavilla, V.R. Pandharipande, R.B. Wiringa, *Nucl. Phys. A* 449 (1986) 219.
- [28] J.-M. Laget, J.F. Lecomte, F. Lefebvre, *Nucl. Phys. A* 370 (1981) 479.
- [29] F.D. Santos, A.M. Eiro, A. Barosso, *Phys. Rev. C* 19 (1979) 238.
- [30] Yu.N. Uzikov, *Fiz. Elem. Chastits At. Yadra* 29 (1998) 1010.
- [31] M. Lacombe, B. Loiseau, R. Vinh Mau, J. Cote, P. Pires, R. de Tourreil, *Phys. Lett. B* 101 (1981) 139.
- [32] P.A.M. Dirac, *Rev. Mod. Phys.* 21 (1949) 392;
S. Weinberg, *Phys. Rev.* 150 (1966) 1313;
L.L. Frankfurt, M.I. Strikman, *Phys. Rep.* 76 (1981) 215.